Heliyon 8 (2022) e11877

Contents lists available at ScienceDirect

Heliyon

journal homepage: www.cell.com/heliyon

Research article

Improvement of driver night vision in foggy environments by structured light projection

Jaime Quintana Benito *, Antonio A. Fernández-Balbuena, Juan Carlos Martínez-Antón, Daniel Váquez Molini

Universidad Complutense de Madrid, Calle Arcos de Jalón, Madrid, 28037, Spain

ARTICLE INFO

Keywords:
Fog visibility scene
Fog and light scattering
Veiling luminance
Fog chamber
Smart lighting
Simulated fog scene

ABSTRACT

Nowadays, fog is still a natural phenomenon that hinders our ability to detect targets, particularly in the field of driving where accidents are increasing. In the literature we find different studies determining the range of visibility, improving the quality of an image, determining the characteristics of fog, etc. In this work we propose the possibility of using a structured lighting system, on which we project the light towards the target, limiting the field lighting. We have developed a scattering light propagation model to simulate and subsequently study the veil luminance, generated by backscattering, to predict the decrease in visibility. This simulation considers the type of fog, the relative orientation of various elements (observer, light source and targets).

We have built a fog chamber to validate the experimental params of the described system.

The results obtained from both the simulation and the experimental measurements demonstrate that it is possible to obtain a high contrast enhancement for viewing a target when illuminated as described.

Clearly, this kind of lighting technology will improve the road safety in foggy night environments. The results of this work can also be extrapolated to any situation in which the visibility of an observer is compromised by the environment, such as heavy rain, smoke from fires, among others.

1. Introduction

Foggy environments present a series of strong disadvantages in perception of the critical causes that make up the environment, adding difficulty in night-time environments in the context of driving, both autonomous and manual [1]. In these environments, due to the attenuation generated by the particles that create fog. When a lighting system projects light onto a scene immersed in fog, this interacts with several elements that make it up, causing the beams to be dispersed and giving rise to a situation of low visibility, which makes it difficult to perceive different elements which are relevant when driving: traffic signs, guidelines, obstacles on the road, etc.

As J.A. Zak mentions, [2], fog is composed of an amalgam of small water droplets and/or ice crystals whose dimensions are between 1 μm and 24 μm. Mie's scattering theory is used to study the scattering phenomenon, since particles that make up fog are usually large particles, as can be seen in Fig. 1. This theory explains the behavior of a beam of light when it strikes a particle, according to X. Li et al. and M.L. Álvarez in [3] & [4] respectively.

As a result of the application of Mie's theory, the phase function is obtained as a result as can be seen in the article by R. N. Mahalati [5]. This expression is the result of solving Maxwell's equations for electromagnetic scattering. It describes the distribution of both the intensity and angular direction of the scattered beam for spherical particles of size comparable or much larger than the incident wavelength, mentioned by Xingcai Li, Li Xie Xiaojing Zheng in their information article [3].

The particles that create fog behave spherically, as they are in suspension, so the phase function is independent of the direction of the incident beam Φ, therefore only the direction of scattering θ varies [5, 6].

$$P(\theta) = \frac{I(\theta)}{I_0}, \tag{1}$$

where I_0 corresponds to the incident beam intensity and $I(\theta)$ corresponds to the scattered intensity as a function of the angle θ, which indicates the direction of scattering, as can be seen in Fig. 2.

* Corresponding author.
E-mail address: jquint01@ucm.es (J. Quintana Benito).

https://doi.org/10.1016/j.heliyon.2022.e11877
Received 15 June 2022; Received in revised form 6 October 2022; Accepted 17 November 2022

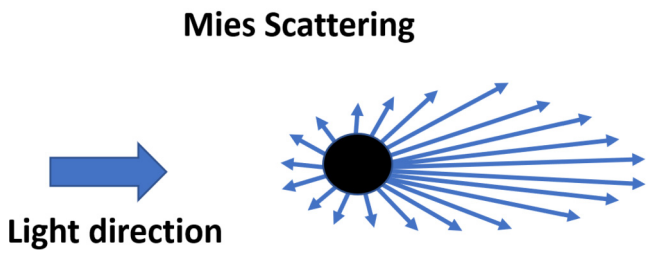

Fig. 1. Beam distribution when incident on a large particle.

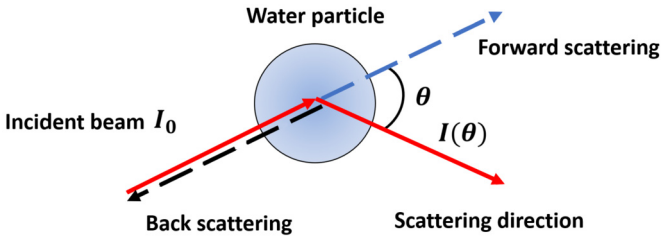

Fig. 2. Diagram of light scattering due to a spherical water particle.

The Lambert-Beer law is used to study the propagation of light. It gives information on how the intensity of a beam varies according to the characteristics of the medium and the distance traveled [7]:

$$I = I_0 e^{-k_{Ex} d}, \tag{2}$$

where I corresponds to the average intensity at a point at a distance d to the origin of the system, I_0 corresponds to the initial intensity of the system, and K_{Ext} is the extinction coefficient of the medium. It is worth mentioning that the extinction coefficient of the medium is made up of the different factors of the medium that affect the propagation of light. In this case, the two most relevant factors are the scattering coefficient α_d and the absorption coefficient α_a, obtaining $K_{Ext} = \alpha_a + \alpha_d$. For this particular case, the absorption coefficient α_a is negligible because it takes values very close to zero for the used wavelengths [8].

As light diffuses through this medium, several factors contribute to a decrease in the visual perceptability of the environment:

1. Attenuation: the loss of intensity of the beam as it passes through the medium. The scattering caused by the fog causes the intensity to decrease by an exponential factor e^{-kd} [9].
2. Halo: this phenomenon occurs when part of the beam reflected from a surface is diffused towards the observer's eye away from the main axis, giving rise to a glow of diffuse light around the reflected beam [9].
3. Veiling luminance: This phenomenon occurs when a part of the transmitted beam is diffused non-uniformly in the main direction. When the beam is reflected, this phenomenon is called retro-reflected veil luminance [9].

In this work, to determine the improvement in the perception of the desired surface when using smart sources, the measurement of contrast using the Weber contrast fraction, a visual perception model used to measure the local contrast of a surface of uniform luminance compared to background is employed [10].

$$c = \frac{\Delta L}{L_{Background}}, \tag{3}$$

where ΔL is the difference between the average luminance of the surface and the average luminance of the near background $L_{Background}$, compared to the average luminance of the background.

In the literature, we have found numerous papers in which they develop systems to determine the range of visibility in foggy environments and fog characteristics [11, 12, 13, 14, 15, 16, 17, 18, 19, 20, 21, 22, 23].

Other works propose vehicle localization systems using sensors that detect vibrations [24], and traffic sign detection using recognition algorithms [25], both in low visibility (fog) situations.

Numerous publications focus on image processing algorithms to obtain clearer images from foggy photographs in order to detect obstacles [1, 26]. We have found algorithms to detect photographs of scenes immersed in fog [27] and thus guarantee a more adequate application of the processing algorithms.

Other works focus on the use of different wavelengths for both visibility enhancement and information transfer in foggy environments [28, 29, 30, 31, 32, 33].

Finally, we have found several articles where statistical studies are made on the risks present during driving in foggy environments and the behavior of drivers in this situation [34, 35].

There are studies about: the improvement of image quality, the determination and/or improvement of the visibility distance, the use of processing algorithms, the variation of the wavelength of the source. Regarding the objective of this work, to improve the visibility using structured light, we have not found relevant articles. The closest is the article by Narasimhan et al. [36], which uses structured light to scan an object submerged in water.

The main objective of this work is to explore and test the possible improvement of visibility and/or contrast in foggy nighttime environments through the use of intelligent light sources, i.e., sources capable of illuminating only the relevant surface necessary for safe driving. In foggy environments, due to light backscattering, factors such as veiled luminance contribute to reduced visual perception. By controlling both the beam intensity and the emission channel, the scattering effects caused by fog are reduced, so that the perception of the desired surface, in particular the contrast of the surface against the background, is improved.

2. Optical modeling of fog environment

2.1. Optical characterization of fog

Fog is an atmospheric phenomenon formed by various concentrations and sizes of water particles and/or ice crystals. In order to develop a generic model of fog, we performed a study of the phase functions for different types of particle sizes using software that allows the extraction of the phase function of a particle by applying Mie scattering theory. The software used is MiePlot. It allows the extraction of intensity data as a function of the angle at which a spherical particle scatters a monochromatic beam [37]. It should be noted that this phase function is defined from 0 to 180 degrees, this is because from 180 to 360 it is symmetrical.

For this work, we have defined the phase function for different wavelengths using the MiePlot data. The spectral will be determined around the visible spectrum [38].

In this case, to get the phase function of a broad-spectrum source, we average the phase functions of all wavelengths for each particle size.

Analyzing the phase functions of several particles of different sizes, we have obtained that the phase functions do not show significant variations. Therefore, it is possible to average them and obtain a generic phase function independent of the droplet size for the simulated system, as shown in Fig. 3.

2.2. Optical simulation of fog

For the study of the veil luminance we have developed a Matlab program that simulates the behavior of light in foggy environments. This program considers different parameters such as the geometrical description of space, the position of the observer and the source, the resolution of the resulting image, as well as varying the spatial projection of the light source beam (Structured light or smart light). It also allows the

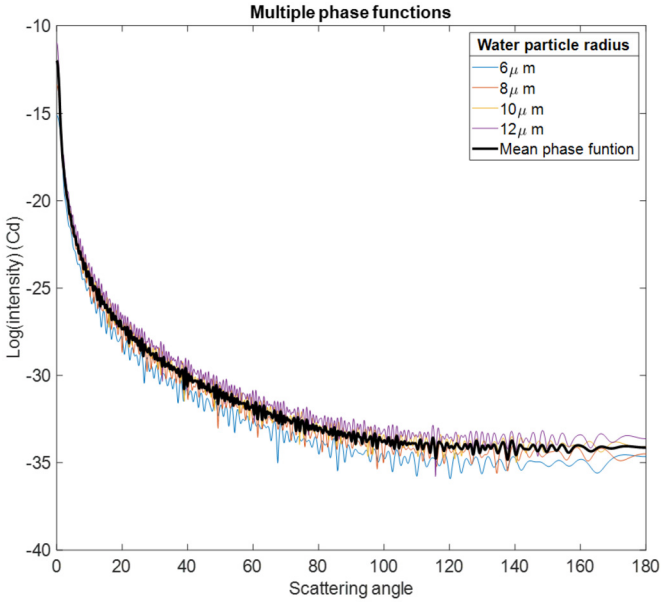

Fig. 3. Representation of multiple phase functions of water particles of different sizes. Determination of the average phase function.

modification of the characteristics of the medium such as the size of the particles and their concentration and the extinction coefficient of the medium [14, 23, 39].

This program develops a volume composed of elementary fog cubes, Fig. 4(a), containing information related to the phase function described above 3. Each represents a backscattering contribution in the direction of the observer. It consists of a cube-shaped matrix structure, which recreates the fog environment. This structure consists of a three-dimensional matrix $nxmxk$, where n and m represent the height and width of the plane and k corresponds to the depth of the cube.

To complete the simulation, we have inserted the source intensity and target reflectance matrix. For these first simulations, the interaction of scattered light from one cube to another is not considered. Once each of the contributions has been ¡ determined, a summation is performed to determine the veil luminance produced by backscattering, as shown in Fig. 4(b), [21].

3. Experimental validation of the optical fog model

We built a fog chamber of dimensions $90x90x220$ cm with MDF boards, Medium Density Fiberboards, and installed two methacrylates in the chamber lids.

To recreate the fog we used a humidifier, adding a solution of water with glycerine at a concentration of $\omega_g = 2\%$, which generates a dense and stable fog while maintaining the refractive index $n' = 1.3351$, similar to that of pure water particles $n_w = 1.3325$. $n' = \omega_w n_w + \omega_g n_g$, where ω_g is the percentage of glycerine with $n_g = 1.4711$ and ω_w is the percentage of remaining solvent, pure water [40].

We use a LASER projector (Casio XJ.15-A251) as a source of illumination to control the illumination of the scene, where a target is placed. We use a video-luminancimeter (Lumican 1300) tp take luminance measures. The measurement range of the Lumicam 1300 is from $0,1$ m Cd/m^2 to 100.000 Cd/m^2 with an average repeatability accuracy of $\pm 0.1\%$.

The measurement process consists of making several luminance measurements of a scene using the lumicam 1300[1] and varying the light beam (structured light) with the projector[2] that is incident on the target[8], which consists of an A4 paper with a black cardboard square of dimensions $7x5$ cm in the center, located at the end of the chamber. The projector illuminates through a 3 mm thick methacrylate window, as shown in the diagram in the Fig. 5. Using luxmeters[3, 7] the value of the extinction coefficient of the fog is determined for each capture, both luxmeters are illuminated with the collimated source[9], the first luxmeter[3] is used to determine the fluctuations of the source and the second luxmeter[7] determines the value used to calculate the extinction coefficient.

The uniformity and stability of the fog is determined to have the time in which the chamber conditions remain unchanged using the following process. Fog is generated for 1 minute. It is stabilized for 30 seconds. A beam is projected and several measurements are made with the lumicam 1300 for 2 minutes. From the obtained measurements a red square is selected, Fig. 6(a), and its luminance is averaged, Fig. 6(b), the obtained value is 0.68 $\frac{\text{Cd}}{\text{m}^2}$.

3.1. Fog chamber measurements

We carry out a process of measuring the luminance received by an observer, which consists of capturing different scenes immersed in fogs of different extinction coefficients in which we place a target. To carry out the measurements, we use the projector, firstly by illuminating the whole scene, wide beam, and secondly, by illuminating only the target, ignoring the cardboard, smart or structured beam.

The extinction coefficient of the generated fog is determined for each scene. Using the Lambert-Beer law (2) and considering the inverse of the law of the square of the distance, we determine the illuminance reaching the sensor considering the conditions of the medium, resulting in the following expression:

$$E' = \frac{I_0 cos(\alpha)}{d^2} e^{-k_{ext} 2d}. \tag{4}$$

If the extinction coefficient is subtracted from the above equation and the illuminance of the source used is considered, it is obtained:

$$K_{ext} = \frac{ln\left(\frac{I_0 cos(\alpha)}{d^2 E'}\right)}{2d} = \frac{ln\left(\frac{E'_0}{E'}\right)}{2d}, \tag{5}$$

where E'_0 corresponds to the illuminance of the source without fog whose value is $E'_0 = 171$ lux, E' corresponds to the illuminance given in a foggy situation and d is the distance from the source to the sensor, in this case, $d = 2.20$ m. From this equation the following extinction coefficients are determined, as can be seen in Table 1:

Table 1. Extinction coefficients.

N° scene	E' (lux)	K_{ext} (m^{-1})
Scene 1	145	0.0374
Scene 2	61	0.2340

We have evaluated the luminance of the images taken for the different extinction coefficients. The luminance of the background with that of the target as a function of the beam type, Figs. 7(a) and 8(a). The mean value of the target luminance is calculated from the luminance profile the ESF values (Edge Spread Function) [41] using the left section indicated in the graph, Figs. 7(b) and 8(b). The contrast is determined using Weber's contrast fraction (3), the results can be seen in Table 2.

3.2. Fog chamber simulation

The experimental situation described in the previous section is simulated using the optical fog Matlab script.

Table 2. Contrast values for each scene.

	Contrast broad beam	Contrast smart beam
Real scene $K_{ext} = 0.0374$ m^{-1}	4.33	21.98
Simulation $K_{ext} = 0.0374$ m^{-1}	**1.37**	**20.40**
Real scene $K_{ext} = 0.2340$ m^{-1}	0.74	3.08
Simulation $K_{ext} = 0.2340$ m^{-1}	**0.14**	**3.64**

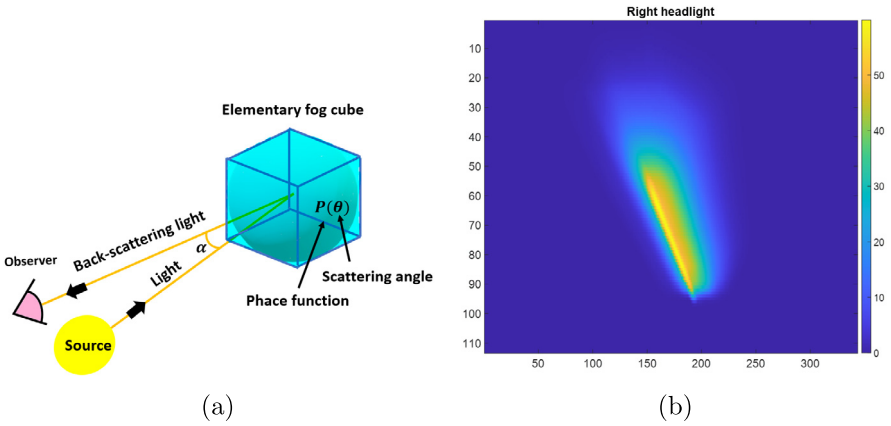

Fig. 4. *a*) Internal outline. *b*) Simulation of how an observer perceives the propagation of light from the right headlight of a vehicle in a fog space of length $z = 15$ m.

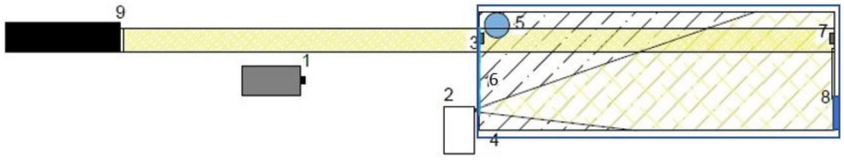

Fig. 5. Video-luminancimeter (Lumicam 1300)[1], Projector (Casio XJ.15-A251)[2], Luxmeter 1[3], Fog chamber[4], Humidifier[5], Methacrylate[6], Luxmeter 2[7], Target[8], Source[9].

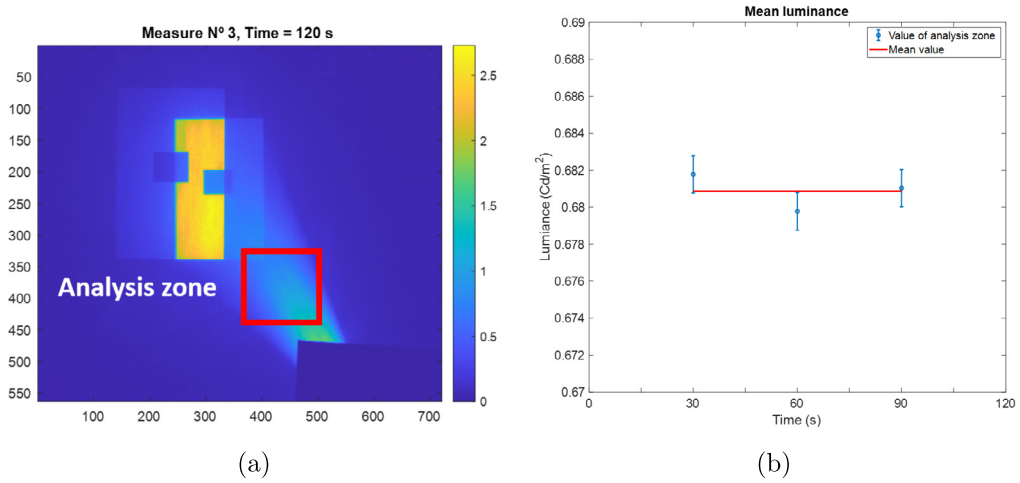

Fig. 6. *a*) Luminance of the fog chamber for stability analysis taken with the Lumicam 1300. *b*) Mean and standard deviation of luminance as a function of elapsed time.

We recreate the conditions of the fog chamber described in the experimental phase: dimensions, the position of the source (projector), of the observer (Lumincam 1300), position and dimensions of the target and the value of the extinction coefficient calculated and the reflectance values of the target.

The results of the simulations can be seen in Figs. 9(a) and 10(a) and the luminance profile in Fig. 9(b) and 10(b).

3.3. Measurement and simulation comparison

Comparing the data obtained both in the real situation and in the simulation, we observe a significant improvement in the perception of the target when the scene is illuminated with a smart source.

4. Simulation of a road fog scene

We recreated the necessary conditions for the situation of a vehicle on the road: dimensions of the space, position of the source (vehicle headlights), of the observer, position and dimensions of the target and the value of the fog extinction coefficient of the scene and the reflectance values of the target, of the road lines and of the asphalt. We generated two situations, one illuminating the entire scene and the other using structured light to illuminate the target.

Several simulations have been performed with different extinction coefficients, Fig. 11(a), 11(b) and 11(d), 11(e). A horizontal section is drawn over the target to analyze the contrast using Weber's contrast fraction (3), calculating the mean luminance values of both the background and the target.

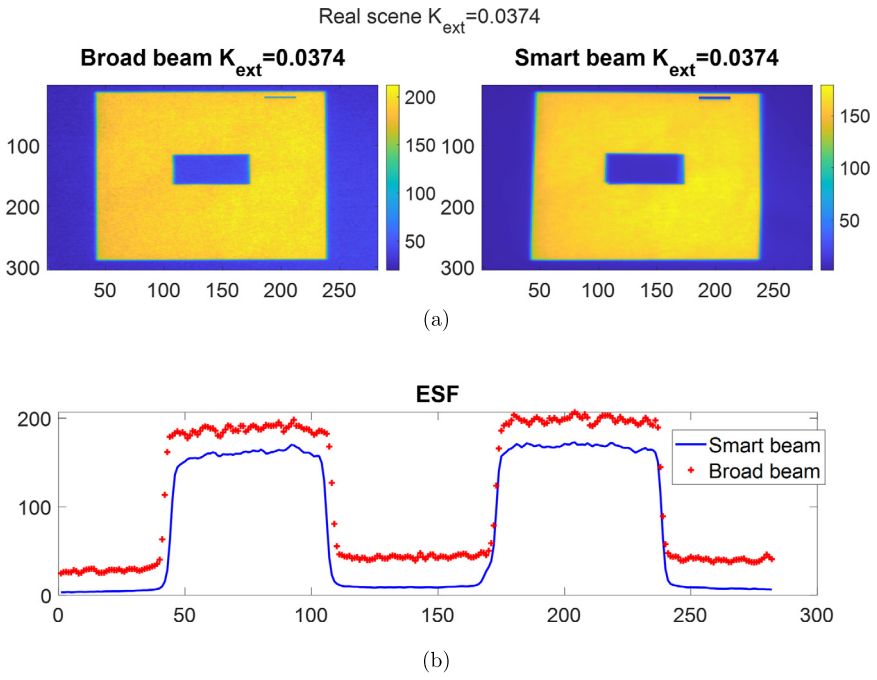

Fig. 7. Luminance of the scene with an extinction coefficient $K_{ext} = 0.0374$ m^{-1}. Fig. 7(a): Images with broad or smart beam. Fig. 7(b): Luminance profile of the previous images at a center horizontal line.

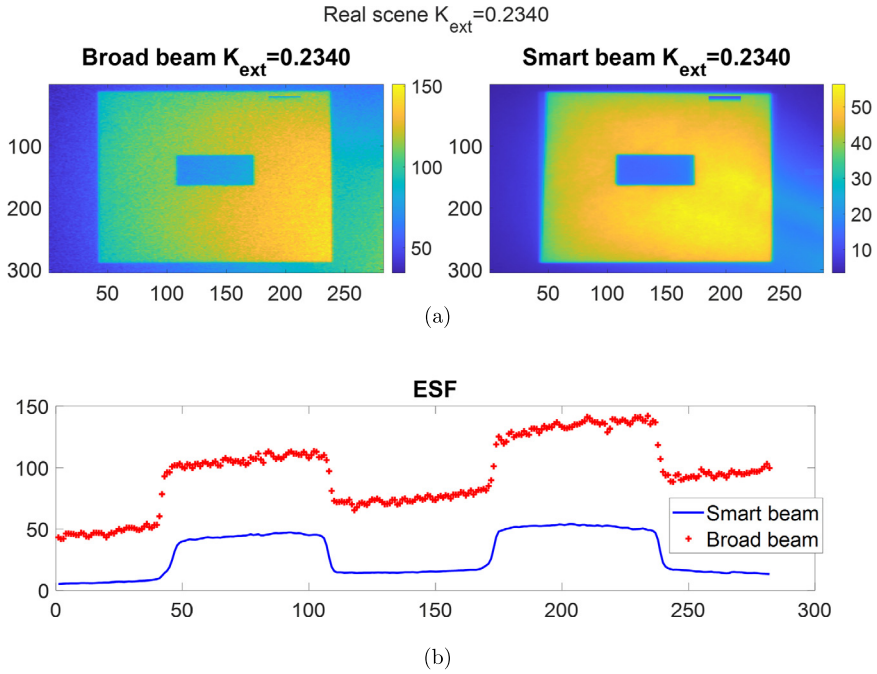

Fig. 8. Luminance of the scene with an extinction coefficient $K_{ext} = 0.2340$ m^{-1}. Fig. 8(a): Images with broad or smart beam. Fig. 8(b): Luminance profile of the previous images at a center horizontal line.

After obtaining the matrix resulting from the projection concerning the observer in Fig. 11. A horizontal section is drawn on the target to analyze the contrast using Weber's contrast fraction (3), calculating the mean luminance values of both the background and the target.

5. Experimental set-up outdoors

An experimental phase was set up in a real foggy environment which allowed the correct parametrization of the models, the evaluation of the detection systems and illumination systems Fig. 12(a).

To obtain the data we used a traffic sign, a LASER projector (Casio X.,15-A251) simulating a vehicle headlight and a CCD to capture the image. We used two lux meters to determine the fog extinction coefficient and a luminance meter to determine light pollution (in this case negligible). The images were processed with Matlab software 12(b). Two situations are generated: illumination of the scene by complete 13(a) and illumination of only the target with a structured or intelligent light 13(b). We proceed to the calculation and evaluation of the contrast for subsequent comparison and parameterization of the model.

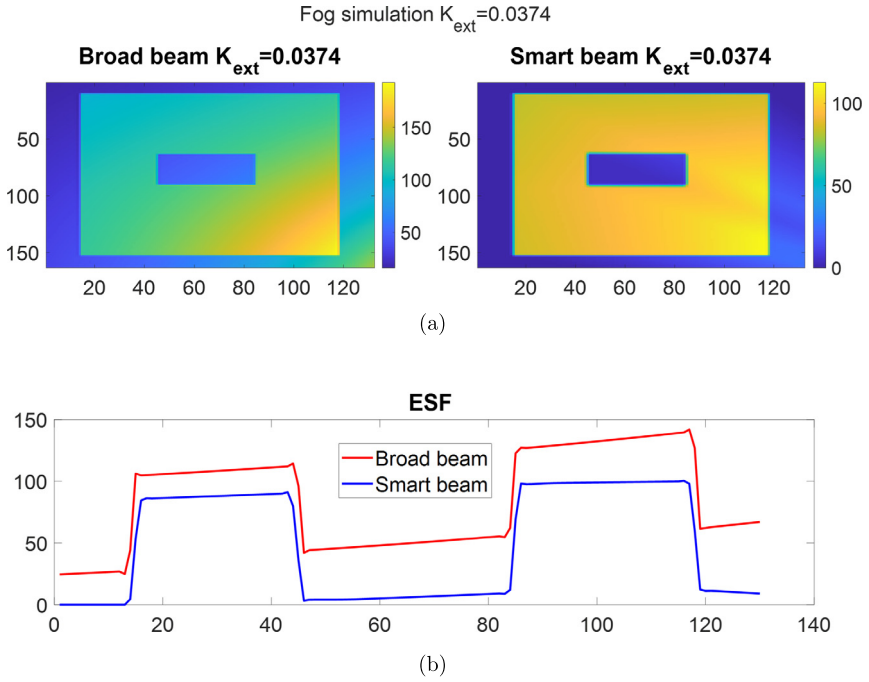

Fig. 9. Luminance of the scene simulated with an extinction coefficient $K_{ext} = 0.0374$ m^{-1}. Fig. 9(a): Images with broad or smart beam. Fig. 9(b): Luminance profile of the previous images at a center horizontal line.

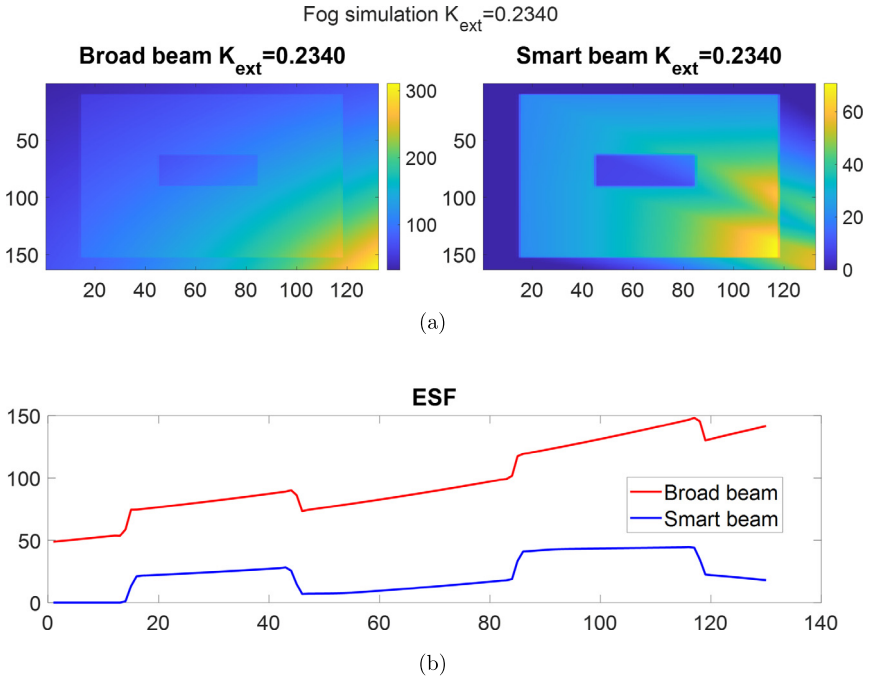

Fig. 10. Luminance of the scene simulated with an extinction coefficient $K_{ext} = 0.2340$ m^{-1}. Fig. 10(a): Images with broad or smart beam. Fig. 10(b): Luminance profile of the previous images at a center horizontal line.

The contrast of the arrow and the circumference with respect to the background is calculated respectively using Weber's contrast fraction (3).

6. Conclusions

Multiple phase functions extracted from Mieplot have been analyzed by varying both the incident wavelength and the water droplet size, reaching the conclusion that for the present work, it is possible to work with an average phase function without having to describe the particular composition of the fog.

Software has been developed to simulate the propagation of light in foggy spaces, offering as a final result the image generated in an optical system (sensor, human eye). This image allows the evaluation of the veil luminance produced by backscattering in this environment, and therefore, to determine the loss of contrast in the detection or perception of a target illuminated in a certain way.

An experimental setup has been developed to recreate a controlled fog environment in the laboratory fog chamber to validate the results

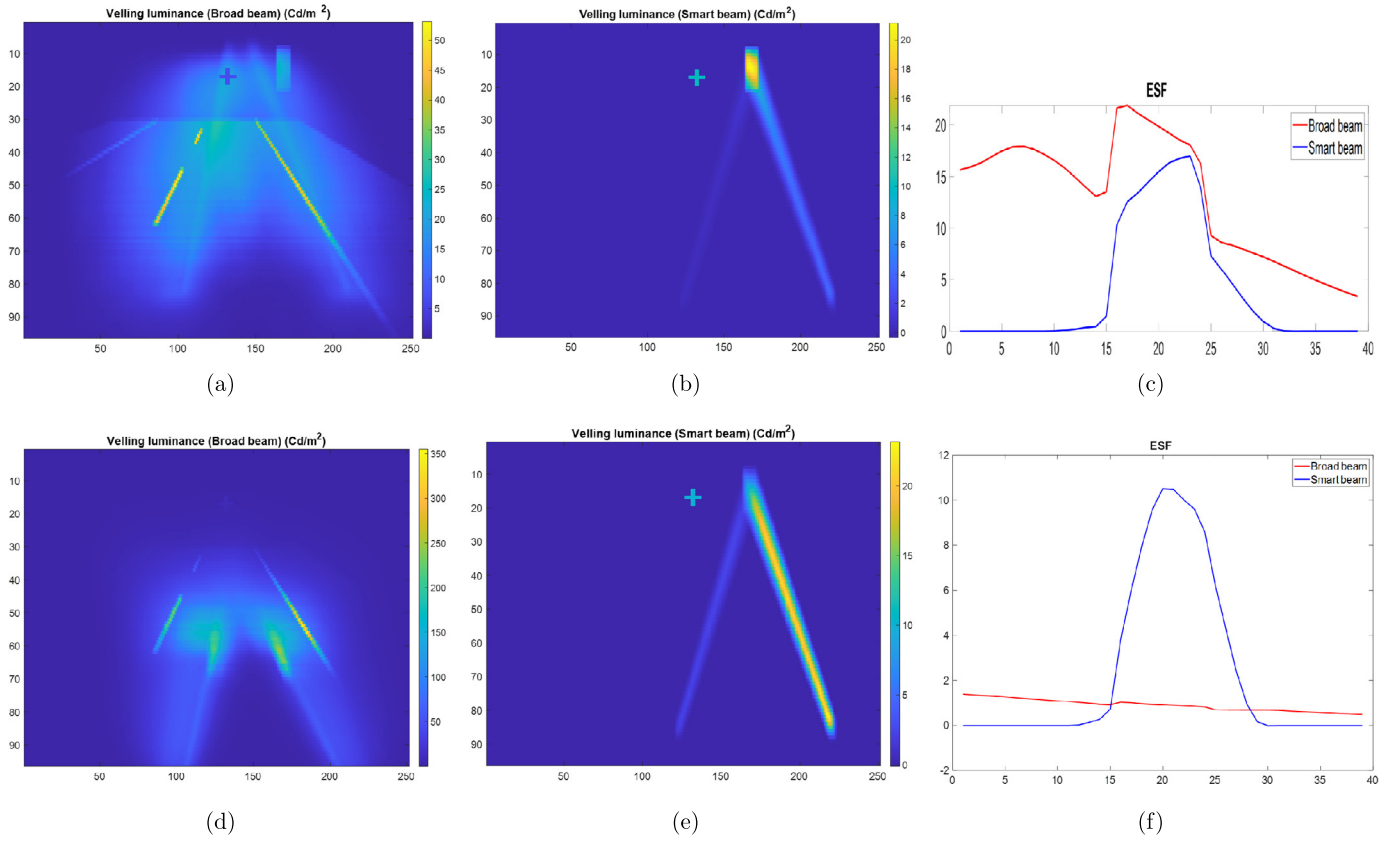

Fig. 11. Projection of the simulations with respect to the observer. The length of the road is 15 m. At 11(a), 11(b) the extinction coefficient is $K_{ext} = 0.01$ m^{-1}. At 11(d), 11(e) the extinction coefficient is $K_{ext} = 0.07$ m^{-1}. Fig. 11(a) and 11(d) correspond to a road illuminated without modifying the beam and 11(b) and 11(e) correspond to the same road but using structured light. 11(c) and 11(f) representation of the horizontal section of both measurements (ESF).

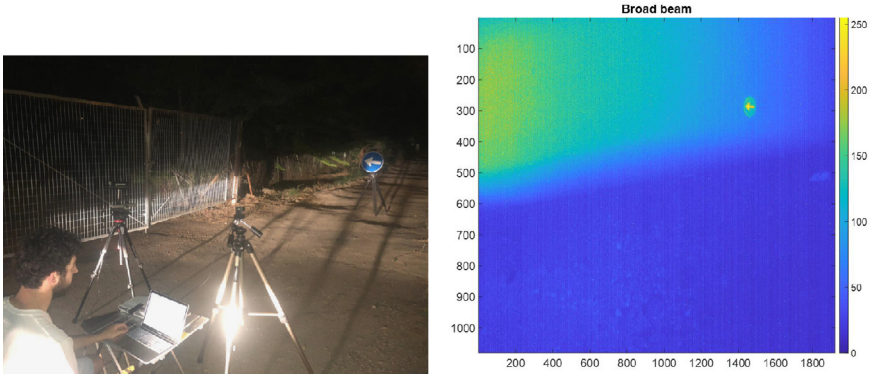

Fig. 12. *A*) Assembly and testing of material. *B*) Images used for the study, illumination of a standard headlight.

obtained in the software simulation. The conditions of the setup were recreated in the simulator: extinction coefficient, source intensity, target, spatial dimensions, etc. As can be seen from the results in Table 2, the simulator gives results similar to reality.

A simulation of a traffic scene generating various types of fog has been carried out to study the behavior of two vehicle headlamps in such circumstances, where again it is observed that by directing the beam to the target the contrast of the target improves notably, as can be seen, in Table 3 for $k_{ext} = 0.01$ m^{-1} and for $k_{ext} = 0.07$ m^{-1}.

An experiment has been designed and carried out in real fog conditions where a traffic signal has been projected using the two forms described above, showing that when illuminated with a smart beam, the contrast $c = 4.91$ improves concerning when illuminated with a broad beam $c = 1.98$ can be seen in Table 4.

Declarations

Author contribution statement

Jaime Quintana Benito, Antonio Álvarez Fernández-Balbuena, Juan Carlos Martínez-Antón & Daniel Váquez Molini: Conceived and designed the experiments; Performed the experiments; Analyzed and interpreted the data; Contributed reagents, materials, analysis tools or data; Wrote the paper.

Funding statement

This work was supported by SEGVAUTO 4.0-, REDES 2018, S2018/EMT-4362.

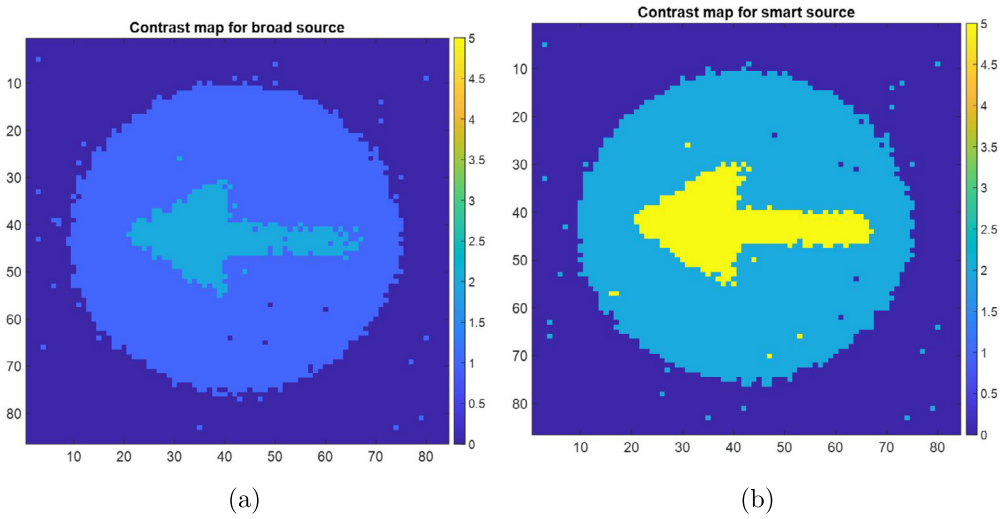

Fig. 13. Contrast map, *a*) Broad headlight *b*) Smart headlight. Correspond to the image in Fig. 12(b).

Table 3. Contrasts obtained from the projections of Figs. 11(c) and 11(f). The following table shows luminance values of both the illuminated target and the background.

$K_{ext} = 0.01$ m^{-1}	Broad source	Smart Source
L_{Target}	19.65	14.47
L_{Background}	11.16	0.89
Contrast	**0.76**	**15.13**

(a)

$K_{ext} = 0.07$ m^{-1}	Broad source	Smart source
L_{Target}	0.92	8.50
L_{Background}	0.88	0.50
Contrast	**0.039**	**15.88**

(b)

Table 4. Contrasts obtained from the signals of Fig. 13.

Arrow	Broad source	Narrow source
L_{Arrow}	226.81	154.59
$L_{Background}$	76.04	26.17
Contrast	**1.98**	**4.91**

Data availability statement

Data included in article/supp. material/referenced in article.

Declaration of interests statement

The authors declare no conflict of interest.

Additional information

No additional information is available for this paper.

References

[1] O. David, N.S. Kopeika, B. Weizer, Range gated active night vision system for automobiles, Appl. Opt. 45 (28) (2006) 7248–7254.

[2] J.A. Zak, Drop size distributions and related properties of fog for five locations measured from aircraft [microform], No. accessed from https://nla.gov.au/nla.catvn4079790, NASA contractor report; NASA CR-4585., Hampton, Va.: [Springfield, Va: National Aeronautics and Space Administration, Langley Research Center; National Technical Informaton Service, distributor 1994].

[3] X. Li, L. Xie, X. Zheng, The comparison between the Mie theory and the Rayleigh approximation to calculate the em scattering by partially charged sand, J. Quant. Spectrosc. Radiat. Transf. 113 (3) (2012) 251–258.

[4] M.L. Alvarez, Nuevos modelos para la caracterización de aerosoles en espectrometría atómica: aplicaciones de la dispersión de la luz láser, PhD thesis, Universidad de Alicante, Carr. de San Vicente del Raspeig, s/n, 03690 San Vicente del Raspeig, Alicante, Feb. 2001.

[5] R.N. Mahalati, J.M. Kahn, Effect of fog on free-space optical links employing imaging receivers, Opt. Express 20 (Jan 2012) 1649–1661.

[6] V.I. Haltrin, One-parameter two-term Henyey-Greenstein phase function for light scattering in seawater, Appl. Opt. 41 (Feb 2002) 1022–1028.

[7] M. Tasumi, Introduction to Experimental Infrared Spectroscopy: Fundamentals and Practical Methods, John Wiley & Sons, 2014.

[8] P. Alonso, Interacción de la radiación con los objetos, Universidad de Murcia, Sept. 2021, https://www.um.es/geograf/sigmur/teledet/.

[9] S.G. Narasimhan, S.K. Nayar, Vision and the atmosphere, Int. J. Comput. Vis. 48 (3) (2002) 233–254.

[10] E. Peli, Contrast in complex images, J. Opt. Soc. Am. A 7 (Oct 1990) 2032–2040.

[11] P. Andre, Improvement of Transport Safety by Control of Fog Production in a Chamber, 2003.

[12] D. Pomerleau, Visibility estimation from a moving vehicle using the Ralph vision system, in: Proceedings of Conference on Intelligent Transportation Systems, IEEE, 1997, pp. 906–911.

[13] N. Hautière, J.-P. Tarel, J. Lavenant, D. Aubert, Automatic fog detection and estimation of visibility distance through use of an onboard camera, Mach. Vis. Appl. 17 (04 2006) 8–20.

[14] S. Lenor, B. Jähne, S. Weber, U. Stopper, An improved model for estimating the meteorological visibility from a road surface luminance curve, in: German Conference on Pattern Recognition, Springer, 2013, pp. 184–193.

[15] H. Chaabani, F. Kamoun, H. Bargaoui, F. Outay, A.-U.-H. Yasar, A neural network approach to visibility range estimation under foggy weather conditions, in: The 8th International Conference on Emerging Ubiquitous Systems and Pervasive Networks (EUSPN 2017) / The 7th International Conference on Current and Future Trends of Information and Communication Technologies in Healthcare (ICTH-2017) / Affiliated Workshops, Proc. Comput. Sci. 113 (2017) 466–471.

[16] V. Cavallo, M. Colomb, J. Doré, Distance perception of vehicle rear lights in fog, Hum. Factors 43 (2001) 442–451.

[17] N. Hautière, R. Labayrade, D. Aubert, Estimation of the visibility distance by stereovision: a generic approach, IEICE Trans. 89-D (01 2006) 2084–2091.

[18] L.R. Bissonnette, G. Roy, N. Roy, Multiple-scattering-based lidar retrieval: method and results of cloud probings, Appl. Opt. 44 (Sep. 2005) 5565–5581.

[19] R. Gallen, A. Cord, N. Hautière, É. Dumont, D. Aubert, Nighttime visibility analysis and estimation method in the presence of dense fog, IEEE Trans. Intell. Transp. Syst. 16 (1) (2014) 310–320.

[20] F. Guo, J. Tang, X. Xiao, Foggy scene rendering based on transmission map estimation, Int. J. Comput. Games Technol. 2014 (2014).

[21] M. Negru, S. Nedevschi, Image based fog detection and visibility estimation for driving assistance systems, in: Proceedings - 2013 IEEE 9th International Conference on Intelligent Computer Communication and Processing, ICCP 2013, 09 2013, pp. 163–168.

[22] E. Dumont, G. Paulmier, P. Lecocq, A. Kemeny, Computational and Experimental Assessment of Real-Time Front-Lighting Simulation in Night-Time Fog, 2004.

[23] E. Dumont, N. Hautière, R. Gallen, A semi-analytic model of fog effects on vision, in: Atmospheric Turbulence, Meteorological Modeling and Aerodynamics, 05 2010.

[24] A.J. Rivas Rodriguez, S. Heinen, W. Mokwa, System concept of a sensor network for vehicular traffic monitoring based on acceleration sensors, Tech. Rep., Lehrstuhl für Integrierte Analogschaltungen und Institut für Halbleitertechnik, 2017.
[25] S.B. Wali, M.A. Abdullah, M.A. Hannan, A. Hussain, S.A. Samad, P.J. Ker, M.B. Mansor, Vision-based traffic sign detection and recognition systems: current trends and challenges, Sensors 19 (9) (2019).
[26] J. Cao, C. Song, S. Song, F. Xiao, S. Peng, Lane detection algorithm for intelligent vehicles in complex road conditions and dynamic environments, Sensors 19 (14) (2019).
[27] K. Jeong, K. Choi, D. Kim, B. Song, Fast fog detection for de-fogging of road driving images, IEICE Trans. Inf. Syst. E101.D (02 2018) 473–480.
[28] M. Verma, V. Yadav, V.D. Kaushik, V.K. Pathak, Addition of yellow frequency in the spectrum for improving vision due to fog, in: 2015 International Conference on Applied and Theoretical Computing and Communication Technology (iCATccT), 2015, pp. 877–881.
[29] K. Fischer, M. Witiw, E. Eisenberg, Optical attenuation in fog at a wavelength of 1.55 micrometers, in: Third International Conference on Fog, Fog Collection and Dew, Atmos. Res. 87 (3) (2008) 252–258.
[30] E. Wainright, H.H. Refai, J.J. Sluss Jr., Wavelength diversity in free-space optics to alleviate fog effects, in: G.S. Mecherle (Ed.), Free-Space Laser Communication Technologies XVII, vol. 5712, International Society for Optics and Photonics, SPIE, 2005, pp. 110–118.
[31] P. Duthon, M. Colomb, F. Bernardin, Light transmission in fog: the influence of wavelength on the extinction coefficient, Appl. Sci. 9 (14) (2019).
[32] B.J. Redman, J.D. van der Laan, K.R. Westlake, J.W. Segal, C.F. LaCasse, A.L. Sanchez, J.B. Wright, Measuring resolution degradation of long-wavelength infrared imagery in fog, Opt. Eng. 58 (Jan. 2019) 051806.
[33] M. Grabner, V. Kvicera, The wavelength dependent model of extinction in fog and haze for free space optical communication, Opt. Express 19 (Feb 2011) 3379–3386.
[34] J.O. Brooks, M.C. Crisler, N. Klein, R. Goodenough, R.W. Beeco, C. Guirl, P.J. Tyler, A. Hilpert, Y. Miller, J. Grygier, et al., Speed choice and driving performance in simulated foggy conditions, Accid. Anal. Prev. 43 (3) (2011) 698–705.
[35] E.R. Boer, S. Caro, V. Cavallo, F. Arcueil, A cybernetic perspective on car following in fog, in: Proceedings of the Fourth International Driving Symposium on Human Factors in Driver Assessment, Training and Vehicle Design, 2007, pp. 9–12.
[36] S. Narasimhan, S. Nayar, B. Sun, S. Koppal, Structured light in scattering media, in: Tenth IEEE International Conference on Computer Vision (ICCV'05), vol. 1, 2005, pp. 420–427.
[37] P. Laven, Mieplot, http://www.philiplaven.com/mieplot.htm, May 2014.
[38] A. Ishimaru, Electromagnetic Wave Propagation, Radiation, and Scattering: from Fundamentals to Applications, John Wiley and Sons, 2017.
[39] E. Dumont, V. Cavallo, Extended photometric model of fog effects on road vision, Transp. Res. Rec. 1862 (01 2004) 77–81.
[40] M.N. Polyanskiy, Refractive index database, https://refractiveindex.info. (Accessed 31 August 2022).
[41] A. Manzanares, M. Calvo, M. Chevalier, V. Lakshminarayanan, Line spread function formulation proposed by w. h. steel: a revision, Appl. Opt. 36 (08 1997) 4362–4366.